Pressure-driven semiconductor-semiconductor transition and its structural origin in oxygen vacancy ordered SrCoO_{2.5}

Fang Hong, Binbin Yue, Zhenxian Liu, Bin Chen, and Ho-Kwang Mao

Pressure-driven semiconductor-semiconductor transition and its structural origin in oxygen vacancy ordered $SrCoO_{2.5}$

Fang Hong[1, 2], Binbin Yue[1, 2, *], Zhenxian Liu[3], Bin Chen[1, *] and Ho-Kwang Mao[1, 3]

[1]*Center for High Pressure Science and Technology Advanced Research, 1690 Cailun Rd. Pudong, Shanghai 201203, P.R. China*

[2]*Advanced Light Source, Lawrence Berkeley National Laboratory, Berkeley, CA 94720, USA*

[3]*Geophysical Laboratory, Carnegie Institution of Washington, Washington, DC 20015, USA*

Email: yuebb@hpstar.ac.cn; chenbin@hpstar.ac.cn

$SrCoO_{2.5}$ has a long-range oxygen vacancy ordering that makes it a promising energy material and catalyst carrier. The study of its electronic properties is vital for its practical applications. Here, we investigate its electronic behavior and lattice structural evolution under high pressure up to 22 GPa using synchrotron infrared spectroscopy and X-ray diffraction. A clear electronic transition from a semiconducting state to another semiconducting state is observed around 7.3 GPa upon compression, based on infrared results. Detailed structural examination shows that this electronic transition is accompanied by a structural phase transition, which occurs between 5.3 and 8.6 GPa, as confirmed by X-ray diffraction. The band gap reduces by ~40% at high pressure compared to ambient conditions. This work demonstrates that the oxygen vacancy ordering in $SrCoO_{2.5}$ can be sustained up to ~8.6 GPa and pressure can narrow the band gap, forcing this unique material to enter into another electronic state with a new crystal structure.

I.   Introduction

Vacancy defects provide active centers where chemical reactions can easily start due to local unbalanced charge distribution [1-3]. Furthermore, some vacancy defects are capable of storing small molecules or ions, which is very useful for energy storage and transfer [4-6]. The vacancies in diamond and silicon have provided a proper system for scientists to control spins or spin qubits, an important research discipline in applied (quantum) physics and computer science, or so-called "quantum computation and communication" [7-11].

Vacancies can even form a superstructure with

long-range ordering rather than disordered distribution, which makes them much more attractive in the fields of catalyst chemistry and energy conversion. $SrCoO_{2.5}$ is one such type of material and it has a long-range order formed by an oxygen vacancy. Currently, there are few reports on the structural change and chemical performance when oxygen atoms enter $SrCoO_{2.5}$ and become $SrCoO_{3-x}$ [12-13]. Ronan Le Toquin *et al.* studied the dynamic process of oxygen intercalation into $SrCoO_{2.5}$ via neutron scattering and X-ray absorption spectroscopy. Two intermediate states, $SrCoO_{2.75}$ and $SrCoO_{2.82,}$ were observed when the oxygen vacancy rate decreased and $SrCoO_{2.82}$ showed clear superstructure reflections from the three-dimensional oxygen ordering. Their work shows clear evidence that $SrCoO_{2.5}$ has a strong oxygen intercalation capability [14]. Hyoungjeen Jeen *et al.* reported the reversible redox behavior of $SrCoO_{2.5}$ and $SrCoO_{3-x}$ epitaxial thin films. The structures of these two phases were tuned using a simple heat treatment near 200-300 ℃. They tested the CO-CO_2 redox reaction using $SrCoO_{2.5}$ thin film around 320℃ and found that $SrCoO_{2.5}$ could be a good redox catalyst for a carbon monoxide oxidation reaction [15].

To explore and extend the potential application of $SrCoO_{2.5}$ in chemical engineering, gas sensors and energy storage, the study of its electronic and structural behavior is crucial. Here, we investigated this unique material using high-pressure infrared

spectroscopy and X-ray diffraction. The diamond anvil cell (DAC) based high-pressure method is a useful and clean tool to change crystal structures and their corresponding physical and/or chemical properties [16-18]. Typical examples of this are solid hydrogen and water, which undergo several phase transitions at room temperature under high pressure, extending our basic understanding of chemistry and physics [19-22]. The electronic behavior of $SrCoO_{2.5}$ under high pressure was examined using synchrotron infrared micro-spectroscopy. Our results show that there is an electronic transition from a semiconducting state to another semiconducting state near 7.3 GPa. To understand the mechanism of this transition, the crystal structure was systematically studied based on synchrotron X-ray diffraction. A structural phase transition was observed between 5.3 and 8.6 GPa, confirming the structural origin of the electronic transition. Furthermore, the compressibility of the low-pressure phase showed quasi-isotropic behavior even when the oxygen vacancy order had a strong preferred orientation.

II. Experiments

The $SrCoO_{2.5}$ sample was synthesized using a solid-state reaction method. A pellet made from stoichiometric amounts of $SrCO_3$ (Sigma-Aldrich 99.9%) and Co_3O_4 (Sigma-Aldrich 99.9%) powders was calcined at 1000℃ for 3 days. The sample was then quenched in liquid nitrogen from this temperature. The infrared experiment was

performed at the U2A infrared microspectroscopy beamline at the National Synchrotron Light Source (NSLS), Brookhaven National Laboratory. For the infrared study, 300-micron culet-type IIa diamonds were used and transmission mode measurements were employed to investigate its optical behavior. A steel gasket was used and a 100-micron sample chamber was drilled by electrical discharge machining (EDM) provided at the U2A beamline. A thin $SrCoO_{2.5}$ sample was placed inside the sample chamber with KBr as a pressure medium. The sample only covered half of the sample chamber and background signals were collected at each pressure point from the other KBr-only half. Two 40*40 micron apertures were used to limit the beam size (upstream apertures were placed in front of the diamond anvil cell so infrared light travelled through the aperture first and then arrived at the sample) and exclude environmental light scattering (downstream apertures were placed behind the diamond anvil cell after light travelled through the sample). Seagle *et. al.* used a similar set-up but only used one aperture [23]. The high-pressure structural evolution was examined by micro X-ray diffraction at Beamline 12.2.2 of the Advanced Light Source (ALS) in Lawrence Berkeley National Laboratory and silicon oil was used as a pressure medium. The incident X-ray energy was 25keV, the wavelength was 0.4959Å and the beam size was 30*30μm. The diffraction patterns were collected from a Mar345 image plate. The pressure was monitored by the

Ruby R1-R2 line shift during both the infrared and X-ray diffraction studies [24-26].

III. Results and discussion
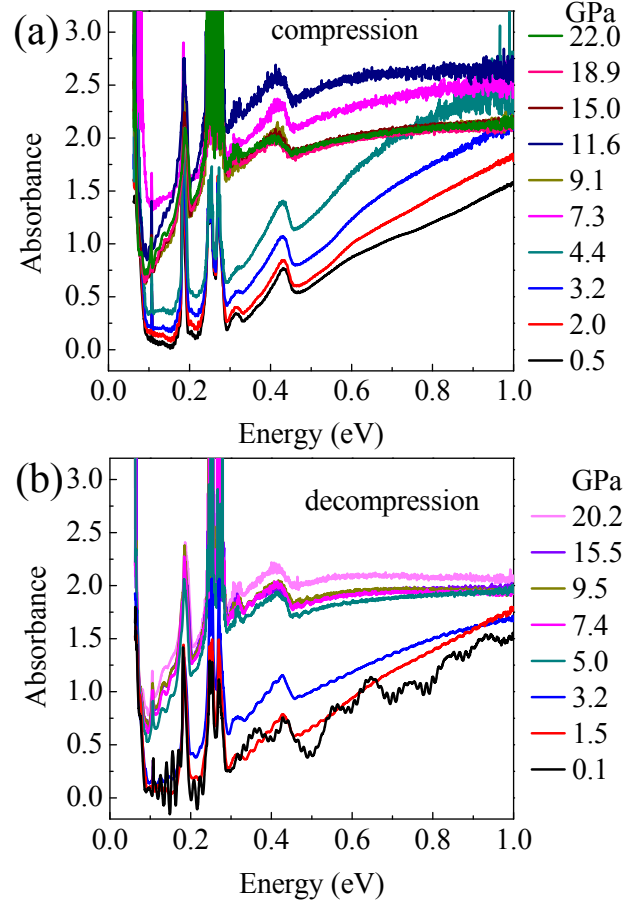
Fig.1 The infrared absorption spectra of $SrCoO_{2.5}$ at selected pressure points: (a) compression and (b) decompression.

The $SrCoO_{2.5}$ sample showed a pale black color due to its strong absorption of visible light, which made studying structural changes under high pressure difficult using Raman spectroscopy. No Raman active modes other than a noisy spectrum were observed. To avoid this problem, we employed infrared spectroscopy to study both the electronic properties and possible structural change of

SrCoO$_{2.5}$ under high pressure. The use of a synchrotron infrared light source allowed efficient collection of good quality spectra with a relatively low signal to noise ratio. Figure 1 displays a series of absorption spectra at some characterized pressure points. The fluctuating absorption near 0.25 eV is due to the diamond absorption background, which was hard to remove completely during the experiment. A wide peak reveals another diamond absorption region near 0.42 eV. At low pressure, the absorbance in the higher energy range was relatively strong compared with the lower energy region. As pressure increased, the absorbance increased over the whole energy range. A distinctively different absorption spectrum was found at 7.3 GPa: absorbance was significantly enhanced below 0.8eV, suggesting an electronic phase transition. Higher pressure did not change the energy dependent absorbance trend and no further qualitative change in the absorption spectra occurred up to the highest investigated pressure.
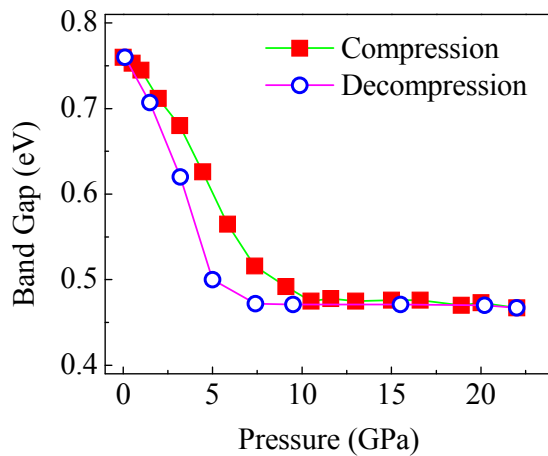

Fig.2 The pressure dependent band gap obtained

from the Tauc relation $(\alpha h v)^2 = A (h v - E g)$, where α is the absorption coefficient, $h v$ is the photo energy and $E g$ is the band gap. There is a clear electronic phase transition near 7.3 GPa. Above this critical pressure, the band gap value is almost constant but shows negative pressure dependence below 7.3 GPa.

The band gap was obtained by fitting the absorption spectra with the Tauc relation [27]. Theoretical calculations predicted that SrCoO$_{2.5}$ is a semiconductor with an indirect band gap [28]. However, our fitting results suggest a direct band gap. We also tried to fit the spectra using an indirect band gap model but the fitting results made no sense. It should be noted that a *Pnma* space group, rather than mostly accepted *Imma* space group, was used in previous calculation [28], which may not provide the accurate result. Hence, further theoretical work is still required. Figure 2 shows the fitting results. The band gap decreased monotonously with pressure up to 10 GPa and did not change much above this pressure during compression. Band gaps were also obtained during decompression and followed a similar trend. In the 0-7.3 GPa pressure range, there was only a small discrepancy between compression and decompression, due to the pressure hysteresis effect. The band gap reduced by ~40% at 7.3 GPa, compared with ambient conditions. Considering the band gap trend during these two processes, we conclude that there is an electronic phase transition

near 7.3 GPa. The electronic band gap of the low-pressure phase was easily tuned by pressure, while the band gap of the high-pressure phase showed no pressure dependent behavior in our current pressure range.
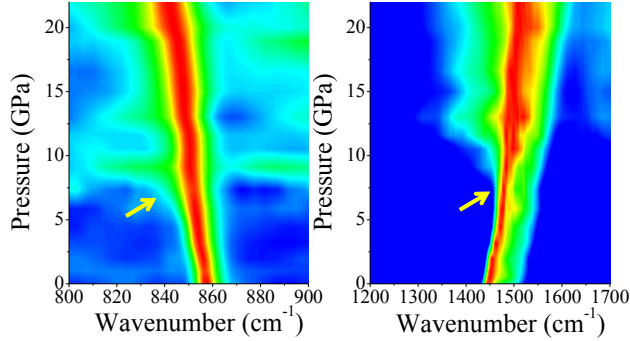
Fig.3 Infrared active modes extracted from the absorption spectra. The broadening of the infrared peaks above ~7.3 GPa is interpreted as a signature of a phase transition.

This electronic phase transition is also confirmed by the damping behavior of two infrared active vibration modes. Figure 3 and Figure 1 show two sharp peaks in the low-energy region around 0.1-0.2 eV. At ambient conditions, the first peak near 860cm^{-1} (equal to 0.107eV) is relatively weak and the second near 1450 cm^{-1} (equal to 0.181eV) is stronger. These two IR active vibration modes are assigned to the ν_2 mode (in-plane bending of the CoO$_6$ octahedron) and the ν_3 mode (asymmetric stretching of the Co-O bond), which are similar to those observed in SrCO$_3$ [29-30]. The low-frequency mode red shifts under high pressure and the high-frequency mode blue shifts. Above ~7.3 GPa, both consistently start to broaden. The damping effect is very strong above 10 GPa, especially for the high-frequency mode.
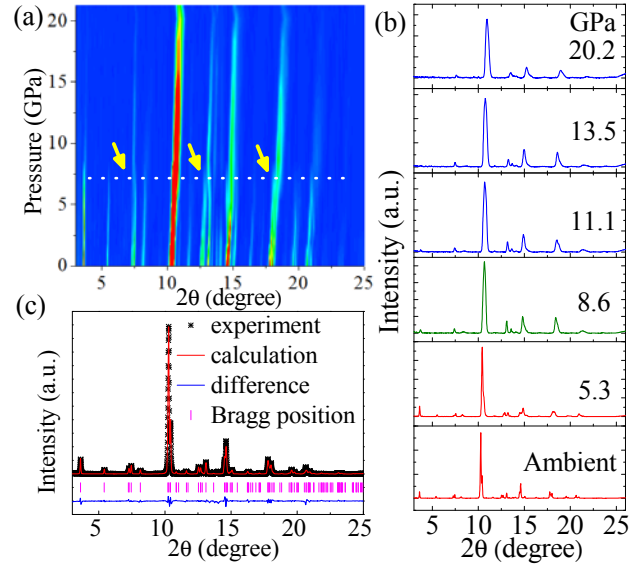

Fig.4 Pressure dependent X-ray diffraction patterns. (a) 2D XRD pattern, yellow arrows are plotted to show the phase transition; (b) selected XRD patterns at various pressures (ambient conditions, 5.3 GPa, 8.6 GPa, 11.1 GPa, 13.5 GPa, and 20.2 GPa); (c) XRD refinement (ambient conditions).

In order to reveal the origin and mechanism of the electronic phase transition, the lattice structural evolution under high pressure was examined *in situ* by synchrotron X-ray micro-diffraction. The pressure dependent XRD pattern is shown in Figure 4(a-b). At ambient conditions, the sample shows a pure brownmillerite phase with space group *Imma* (Figure 4c). When the pressure increased, all diffraction peaks shifted to a higher angle, suggesting that the lattice parameter and volume also contracted. Between 5.3 GPa and 8.6 GPa, some peaks were strongly suppressed indicating a

structural phase transition, which is well matched with the electronic phase transition pressure determined by the infrared absorption spectra. The peak ($2\theta \approx 3.6°$) contributed by the oxygen vacancy ordering was also suppressed above this critical phase transition pressure. Hence, the structure of $SrCoO_{2.5}$ was stable up to ~8.6 GPa. Above this transition pressure, *DicVol04* software assigns the structure to another orthorhombic structure with space group *P222*. However, this high-pressure phase is somewhat difficult to determine due to the weak and broadened diffraction signal. According to previous calculations, the structure with space group *Pnma* is possibly a low-temperature phase for $SrCoO_{2.5}$ and sometimes effects of high pressure on the crystal structure are qualitatively comparable to those induced by low temperature. Similar systems, such as $CaFeO_{2.5}$, can exist in the form of a *Pnma* structure [28, 31]. Therefore, it is possible that the high-pressure phase has a *Pnma* structure. However, based on the peak position information, the only possible structure is *P222* rather than *Pnma* and other orthorhombic structures. We also considered the possibility of a cubic phase, which is the stable structure found in $SrCoO_3$ [32]. However, the cubic phase was finally excluded due to the large mismatch of the Bragg positions, despite their patterns looking quite similar. Further study is still required to clarify the structural details in the high-pressure phase.

To further test the structural stability of the brownmillerite phase, the compressibility was examined by comparing the pressure dependent lattice parameters along the *a*, *b*, and *c* directions. The results are presented in Figure 5 and the volume change is also presented for reference. All three lattice parameters show a similar trend with pressure. Birch-Murnaghan equation of state (EOS) analysis (K'=4.0, fixed) gives the linear modulus: K_a=103.6±9.6 GPa, K_b=106.1±9.8 GPa, and K_c=90.9±8.4 GPa. Hence, there is no strong anisotropic compressibility behavior. The bulk modulus is K_B=99.9±9.3 GPa (K_B'=4.0, fixed). This suggests that the lattice structure of the oxygen vacancy ordered $SrCoO_{2.5}$ is very stable and shows quasi-isotropic compressibility in the low-pressure range from ambient conditions to ~7.3 GPa (confirmed by IR and XRD experiments). At 8.6 GPa, the structure became unstable.
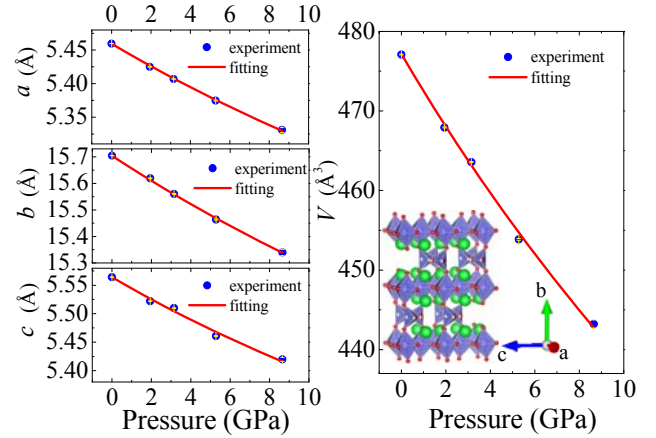
Fig.5 The lattice parameter and volume change under high pressure for the low-pressure phase. Both the lattice parameters and volume decrease monotonously with pressure. The compressibility of a, b, and c is very similar and there is no clear

anisotropic dependence. Insert: the atomic structure of $SrCoO_{2.5}$

IV. Conclusion

The electronic and structural behavior of $SrCoO_{2.5}$ under high pressure was investigated by synchrotron infrared micro-spectroscopy and X-ray diffraction. The infrared spectroscopy experiment revealed an electronic transition from a semiconducting state to another semiconducting state near 7.3 GPa. The XRD-based structural investigation showed a structural phase transition between 5.3 and 8.6 GPa, which suggests the observed electronic transition had a structural origin. In the low-pressure phase, the band gap decreased when the pressure increased. For the high-pressure phase, the band gap had weak pressure dependence. In addition, the lattice parameters of the low-pressure phase showed unexpected quasi-isotropic compressibility, which could be advantageous for its application in the fields of energy storage, catalyst carriers, and gas sensors at both ambient and extreme conditions.

References

[1]   X. Liu, K. Zhou, L. Wang, B. Wang, Y. Li, J. Am. Chem. Soc., **131**, 3140 (2009).

[2]   H. Gunaydin, K. N. Houk, V. Ozoliņš, Proc. Natl. Acad. Sci., **105**, 3673 (2008).

[3]   Z. A. Feng, F. El Gabaly, X. Ye, Z.-X. Shen, W. C. Chueh, Nature Commun., **5**, 5374 (2014).

[4]   X. Li, Y. Feng, M. Li, W. Li, H. Wei, D. Song, Adv. Funct. Mater., **25**, 6858 (2015).

[5]   F. T. Li, J. Ran, M. Jaroniec, S. Z. Qiao, Nanoscale, **7**, 17590 (2015).

[6]   Y. Xu, M. Zhou, X. Wang, C. Wang, L. Liang, F. Grote, M. Wu, Y. Mi, Y. Lei, Angew. Chem. Int. Ed., **54**, 8768 (2015).

[7]   C. G. Yale, F. J. Heremans, B. B. Zhou, A. Auer, G. Burkard, D. D. Awschalom, Nature Photonics, **10**, 184 (2016).

[8]   H. Kosaka, N. Niikura, Phys. Rev. Lett., **114**, 053603 (2015).

[9] S. Kolkowitz, A. Safira, A. A. High, R. C. Devlin, S. Choi, Q. P. Unterreithmeier, D. Patterson, A. S. Zibrov, V. E. Manucharyan, H. Park, M. D. Lukin, Science, **347**, 1129 (2015).

[10] J. J. Pla, K. Y. Tan, J. P. Dehollain, W. H. Lim, J. J. L. Morton, F. A. Zwanenburg, D. N. Jamieson, A. S. Dzurak, A. Morello, Nature, **496**, 334 (2013).

[11] J. J. Pla, K. Y. Tan, J. P. Dehollain, W. H. Lim, J. J. L. Morton, D. N. Jamieson, A. S. Dzurak, A. Morello, Nature, **489**, 541 (2012).

[12] H. Jeen, W. S. Choi, J. W. Freeland, H. Ohta, C. U. Jung, H. N. Lee, Adv. Mater., **25**, 3651 (2013).

[13] H. Jeen, Z. Bi, W. S. Choi, M. F. Chisholm, C. A. Bridges, M. P. Paranthaman, H. N. Lee, Adv. Mater., **25**, 6459 (2013).

[14] R. Le Toquin, W. Paulus, A. Cousson, C. Prestipino, C. Lamberti, J. Am. Chem. Soc., **128**, 13161 (2006).

[15] H. Jeen, W. S. Choi, M. D. Biegalski, C. M. Folkman, I. C. Tung, D. D. Fong, J. W. Freeland, D. Shin, H. Ohta, M. F. Chisholm, H. N. Lee, Nat. Mater., **12**, 1057 (2013).

[16] F. Hong, B. Yue, Z. Cheng, M. Kunz, B. Chen, H.-K. Mao, Appl. Phys. Lett., **109**, 041907 (2016).

[17] F. Hong, B. Yue, N. Hirao, G. Ren, B. Chen, H.-K. Mao, Appl. Phys. Lett., **109**, 241904 (2016).

[18] B. Yue, F. Hong, S. Merkel, D. Tan, J. Yan, B. Chen, H.-K. Mao, Phys. Rev. Lett., **117**, 135701 (2016).

[19] C. S. Zha, R. E. Cohen, H. K. Mao, R. J. Hemley, Proc. Natl. Acad. Sci. U. S. A., **111**, 4792 (2014).

[20] B. Kamb, B. L. Davis, Proc. Natl. Acad. Sci., **52**, 1433 (1964).

[21] I.-M. Chou, J. G. Blank, A. F. Goncharov, H.-k. Mao, R. J. Hemley, Science, **281**, 809 (1998).

[22] C. Lobban, J. L. Finney, W. F. Kuhs, Nature, **391**, 268 (1998).

[23] C. T. Seagle, D. L. Heinz, Z. Liu, R. J. Hemley, Appl. Opt., **48**, 545 (2009).

[24] H. K. Mao, P. M. Bell, Science, **191**, 851 (1976).

[25] J. H. Eggert, K. A. Goettel, I. F. Silvera, Phys. Rev. B, **40**, 5724 (1989).

[26] J. H. Eggert, K. A. Goettel, I. F. Silvera, Phys. Rev. B, **40**, 5733 (1989).

[27] J. Tauc, A. Menth, J. Non-Cryst. Solids, **8–10**, 569 (1972).

[28] H.-P. Wu, K.-M. Deng, F.-L. Hu, W.-S. Tan, C.-M. Tang, Q.-X. Li, Chin. Phys. Lett., **26**, 017105 (2009).

[29] B. Sreedhar, M. Sulochana, C. S. Vani, D. K. Devi, N. V. S. Naidu, Eur. Chem. Bull., **3**, 234 (2014).

[30] S. Makhloufi, M. Omari, J. Inorg. Organomet. Polym., **26**, 32 (2016).

[31] M. a. I. Gómez, J. A. de Morán, R. E. Carbonio, P. J. Aymonino, J. Solid State Chem., **142**, 138 (1999).

[32] J. Y. Yang, C. Terakura, M. Medarde, J. S. White, D. Sheptyakov, X. Z. Yan, N. N. Li, W. G. Yang, H. L. Xia, J. H. Dai, Y. Y. Yin, Y. Y. Jiao, J. G. Cheng, Y. L. Bu, Q. F. Zhang, X. D. Li, C. Q. Jin, Y. Taguchi, Y. Tokura, Y. W. Long, Phys. Rev. B, **92**, 195147 (2015).